

Few-Shot Learning Pipeline for Monkeypox Skin Disease Classification Using CNN Feature Extractors

Md. Safirur Rashid¹, Sabbir Ahmed¹, Muhammad Usama Islam^{1,2}, Sumona Hoque Mumu³, and Md. Hasanul Kabir¹

- ¹ Department of Computer Science and Engineering, Islamic University of Technology, Gazipur, Bangladesh
{safirurrashid, sabbirahmed, usamaislam, hasanul}@iut-dhaka.edu
- ² Management Information Systems, Metropolitan State University, Minnesota, USA
muhammadusama.islam@metrostate.edu
- ³ School of Kinesiology, University of Louisiana at Lafayette, LA, USA
sumona-hoque.mumul@louisiana.edu

Abstract. Despite the strong performance of Convolutional Neural Networks (CNNs) in disease classification, their effectiveness often depends on access to large annotated datasets, which is an impractical requirement for emerging or rare conditions such as Monkeypox. To overcome this limitation, we propose a few-shot learning (FSL) framework that employs SimpleShot, a lightweight, non-parametric, inductive classifier, for Monkeypox and pox-like skin disease recognition from limited labeled examples. The proposed pipeline passes the skin lesion images through a frozen, pretrained CNN backbone to obtain feature embeddings, which are then classified via SimpleShot using nearest-centroid comparisons in a normalized embedding space. We systematically benchmark six widely used CNN backbones as feature extractors under consistent experimental settings, enabling fair comparison. Experiments on three publicly available datasets (MSLD v1.0, MSID, and MSLD v2.0) are conducted across 2-way, 4-way, and 6-way tasks with 1-shot, 5-shot, and 10-shot configurations. Among all models, MobileNetV2_100 consistently achieves the highest accuracy. In addition, we present a cross-dataset evaluation for Monkeypox classification, revealing that binary Mpox-vs-Others transfer remains comparatively stable while multi-class performance degrades significantly under domain shift. Together, these results demonstrate the practical utility of combining inductive FSL methods with lightweight CNN backbones and highlight the importance of domain robustness for reliable real-world clinical deployment.

Keywords: Skin Lesion Diagnosis · SimpleShot · Lightweight Models · Medical Image Analysis · Low-Resource Learning

1 Introduction

Monkeypox is a re-emerging zoonotic disease caused by the Monkeypox virus (MPXV), a member of the *Orthopoxvirus* genus [37]. It clinically manifests with skin lesions that

are visually similar to other pox-like illnesses such as Chickenpox, Measles, and Cowpox, making accurate clinical diagnosis particularly challenging in early stages or in low-resource settings [8,45]. With the global resurgence of Monkeypox cases especially in non-endemic regions there is an increasing need for automated diagnostic systems that can aid in triage and early detection [36,38,40,41].

The automatic feature learning capability of modern deep learning models has revolutionized the field of artificial intelligence, driving state-of-the-art solutions across diverse downstream tasks in computer vision [5,20,22,26,42], speech recognition [13,54], natural language processing [6,35], and related domains [4,11,12,29]. Within medical data analysis in particular, these advances have enabled automated systems to achieve expert-level performance in tasks once considered uniquely dependent on clinical expertise [1,7,30,31,49]. Deep learning (DL), especially convolutional neural networks (CNNs), now serves as the backbone of medical image understanding, powering systems for dermatology, radiology, and histopathology [15,27]. In skin disease classification, CNNs trained on large-scale datasets such as ISIC [16] have already reached dermatologist-level accuracy [28]. Motivated by this success, recent works have explored applying DL to Monkeypox detection [14,19,21,32]. For instance, MonkeyNet [14] leverages a DenseNet backbone to discriminate pox-like skin conditions with high accuracy, while others integrate attention mechanisms [21] or self-supervised learning strategies [19]. More recently, federated learning approaches have been introduced to mitigate data-sharing and privacy challenges [33].

Despite promising results, most existing approaches primarily adopt conventional supervised learning pipelines, often supplemented with data augmentation strategies to artificially expand the training set [25]. While such methods can provide marginal improvements, they remain fundamentally constrained by the availability and diversity of labeled data. In the case of Monkeypox, datasets are still relatively small, highly imbalanced, and difficult to curate due to the challenges of obtaining clinically verified images across different stages of infection, varying skin tones, and real-world conditions. This scarcity not only limits the generalizability of supervised models but also amplifies risks of overfitting, where models may inadvertently exploit spurious correlations instead of learning robust disease-relevant features [9,10]. These limitations highlight the need for alternative paradigms, such as few-shot learning, aiming to achieve strong generalization under low-data regimes by leveraging transferable representations.

Few-shot learning (FSL) has emerged as a powerful paradigm for addressing extreme data scarcity by enabling models to generalize from only a handful of labeled examples per class [2,3]. Comprehensive surveys have chronicled its evolution from early metric-learning approaches to meta-learning and self-supervised methods, emphasizing its growing role in low-resource machine learning scenarios [51,53]. In the medical domain, FSL has shown considerable success in tasks such as disease classification [47], hyperspectral imaging [34], and medical image segmentation [39], retinal imaging [47], cancer detection [18], and multimodal classification [55] reducing the need for large annotated datasets while retaining strong generalization capabilities. However, FSL remains largely underexplored in the context of Monkeypox and other pox-like skin diseases. While some recent works have introduced tailored few-shot

pipelines that incorporate domain adaptation via pretrained encoder fine-tuning [17], these approaches often rely on access to auxiliary datasets.

In contrast, our work explores a purer inductive few-shot learning setup, eschewing domain adaptation entirely by pairing frozen convolutional feature extractors with a non-parametric classifier to assess generalization under low-data constraints. Our proposed FSL pipeline is tailored for Monkeypox and pox-like skin disease classification, centered around the SimpleShot algorithm [52], a robust prototype-based algorithm that performs nearest-centroid classification in a normalized embedding space. We adopt the SimpleShot algorithm not only for its simplicity and efficiency, but also because it achieves strong empirical performance on standard benchmarks without requiring costly meta-training, making it ideal for low-resource clinical settings.

To the best of our knowledge, this is the first systematic evaluation of CNN-based feature extractors for Monkeypox classification using a standardized few-shot pipeline. Our contribution lies in establishing a reproducible framework, centered around the SimpleShot algorithm, in which we benchmark six widely used CNN backbones as frozen feature encoders. Unlike prior efforts focusing on either novel FSL algorithms or fully supervised deep learning approaches, we shift focus toward understanding which CNN backbones are most effective for low-data skin disease classification, and how this choice influences model generalization, efficiency, and clinical applicability.

To evaluate our SimpleShot-centered pipeline, we benchmark six widely used pretrained CNNs, VGG16 [46], InceptionV3 [48], ResNet50 [23], DenseNet121 [24], MobileNetV2_100 [43], and EfficientNet_B1 [50] as frozen feature extractors, feeding their output embeddings directly into the SimpleShot classifier to isolate the impact of backbone choice. Experiments are conducted on three publicly available skin lesion datasets, MSLD v1.0 [10], MSID [14], and MSLD v2.0 [9] across 2-way, 4-way, and 6-way classification tasks under 1-shot, 5-shot, and 10-shot configurations. Each setup is evaluated over 100 few-shot episodes with 50 query samples, and performance is reported as mean accuracy with 95% confidence intervals. Results show that MobileNetV2_100 achieves the best balance between accuracy and computational efficiency, while increasing support size consistently improves performance. Class-level analysis reveals higher confusion among visually similar conditions, such as Monkeypox and Chickenpox, reinforcing the need for strong feature encoders in low-data clinical environments. The key contributions of this work are as follows:

- We introduce a simple, scalable, and effective few-shot learning pipeline for Monkeypox skin disease classification, built entirely around the SimpleShot algorithm.
- We benchmark six widely used CNN backbones as feature extractors within this pipeline and identify MobileNetV2_100 as the most effective architecture.
- Upon benchmarking on three datasets, we analyze the impact of class count, support size, and disease similarity on classification accuracy, providing practical insights for deploying FSL models in real-world clinical screening scenarios.
- We conduct a comprehensive cross-dataset evaluation for Monkeypox skin disease classification, showing that binary Mpox-vs-Others transfer remains relatively stable (63–68%), whereas multi-class generalization degrades significantly under domain shift, highlighting the need for domain-adaptive FSL strategies to ensure reliable clinical deployment across diverse data sources.

2 Methodology

This study proposes a streamlined and reproducible FSL pipeline for Monkeypox and pox-like skin disease classification, with a specific focus on identifying the most effective convolutional neural network (CNN) backbone for feature extraction with limited data. At the core of our pipeline lies SimpleShot [52], a lightweight and efficient prototype-based FSL algorithm that classifies query samples by computing distances to class centroids in a normalized embedding space. We adopt SimpleShot not only for its speed and simplicity, but also because it eliminates the need for costly meta-training and enables direct benchmarking of backbone quality. The overall experimental workflow is illustrated in Figure 1, showing the pipeline from image input through CNN-based embedding extraction and final classification via SimpleShot.

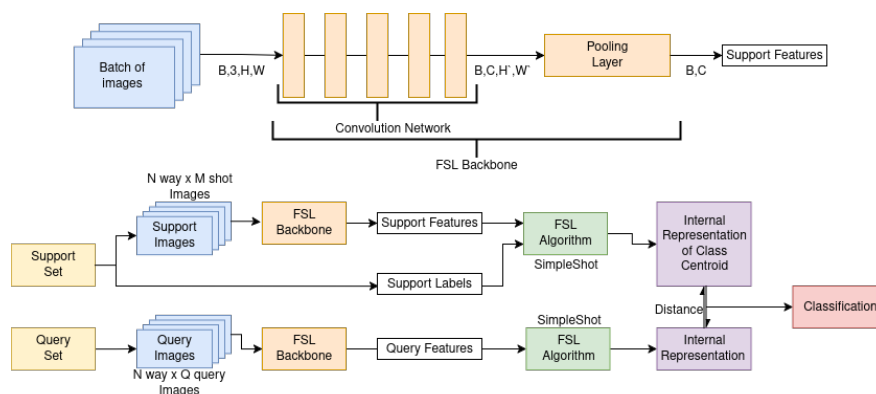


Fig. 1: Overview of the proposed pipeline: input images are processed by a frozen CNN backbone to extract feature embeddings, which are then classified using SimpleShot in an N -way M -shot setting.

2.1 Dataset Overview

We utilized three publicly available skin lesion datasets, MSLD v1.0 [10], MSID [14], and MSLD v2.0 [9] that differ in size, class diversity, and visual complexity. All experiments are conducted exclusively on the original, unaugmented versions to avoid bias and ensure consistency in backbone evaluation. We evaluate model performance across 2-way, 4-way, and 6-way classification scenarios using M -shot settings with $M \in \{1, 5, 10\}$ and a fixed query set of 50 samples per episode. Each configuration is repeated over 100 randomly sampled tasks to ensure statistical robustness. Results are reported as mean accuracy along with 95% confidence intervals.

Monkeypox Skin Lesion Dataset v1.0 (MSLD v1.0) : MSLD v1.0, released during the early stages of the 2022 Monkeypox outbreak [10], is a binary classification dataset comprising 228 clinical images: 102 of Monkeypox and 126 from a merged ‘Others’ class that includes Chickenpox and Measles. Figure 2 shows a sample from each class, illustrating the diagnostic challenge posed by the visual overlap between Monkeypox and other viral skin diseases.

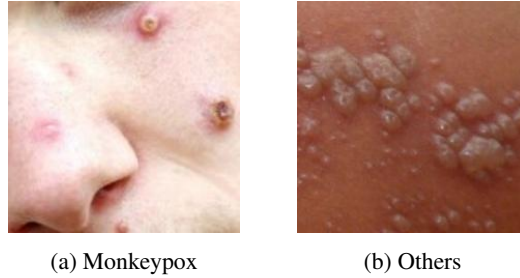


Fig. 2: Example images from the MSLD v1.0 dataset [10]. (a) Monkeypox: deep-seated pustules with defined borders and occasional central umbilication. (b) Chickenpox: clusters of small vesicles on an erythematous base, more superficial and variable in size, sometimes resembling shingles. Such features can overlap with early Monkeypox, thereby increasing diagnostic complexity.

Images were sourced from publicly available repositories and subjected to a two-stage quality control process, involving duplicate removal and clinical verification via manual screening and Google Reverse Image Search. Although subsequent studies have expanded this dataset with augmented samples, our work confines evaluation strictly to the original collection to prevent potential data leakage. Despite its modest scale, MSLD v1.0 serves as a valuable low-shot, 2-way classification benchmark. The heterogeneous composition of the *Others* class introduces significant intra-class variability, simulating diagnostic ambiguity and providing a challenging testbed for early screening scenarios.

Monkeypox Skin Lesion Dataset (MSLD v2.0): MSLD v2.0 is a six-class dataset comprising 755 high-quality clinical and dermoscopic skin images from 541 unique patients. The classes include Monkeypox (284), Chickenpox (75), Measles (55), Cowpox (66), Hand-Foot-Mouth Disease (161), and Healthy skin (114), collectively covering a broad spectrum of visually overlapping conditions relevant for differential diagnosis.

Developed by Ali *et al.* [9], MSLD v2.0 extends earlier efforts [10, 14] by significantly enlarging the sample base. All images were collected via web scraping, de-identified to protect patient privacy, and clinically validated by infectious disease experts. Although the full dataset includes over 39,000 augmented samples, our experiments are conducted exclusively on the original 755 images. Representative examples are shown in Figure 3, highlighting the strong visual similarity among conditions such as Monkeypox, Chickenpox, and Cowpox.

Overall, MSLD v2.0 presents a challenging 6-way classification benchmark characterized by class imbalance and substantial inter-class ambiguity, particularly among pox-like diseases. Its clinical diversity and diagnostic complexity make it a valuable testbed for assessing backbone generalization and robustness in FSL frameworks.

Monkeypox Skin Images Dataset (MSID): This dataset was curated by Bala *et al.* [14], consisting of 770 clinical images grouped into four diagnostic classes: Monkeypox (279), Chickenpox (107), Measles (91), and Healthy (293). The samples were sourced from medical literature, dermatological atlases, and publicly available image repositories, with a focus on diseases commonly misdiagnosed due to visual similarity.

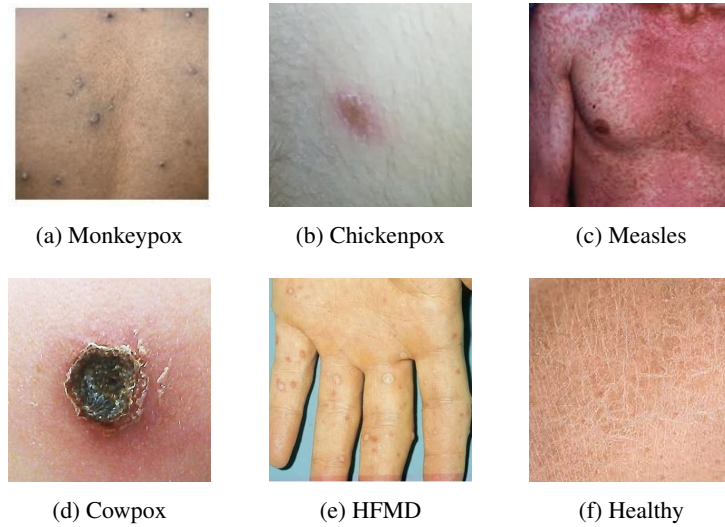


Fig. 3: Example images from the MSLD v2.0 [9] dataset. (a) Monkeypox: well-circumscribed pustules with central umbilication. (b) Chickenpox: superficial vesicles on red bases at mixed stages. (c) Measles: widespread confluent maculopapular rash. (d) Cowpox: necrotic lesion with central eschar. (e) HFMD: vesicles localized to palms, soles, or mucosa. (f) Healthy: normal skin without lesions, serving as control.

Representative class-wise samples are presented in Figure 4, highlighting both inter-class similarities and visual variance in skin tone, lighting, and lesion type.

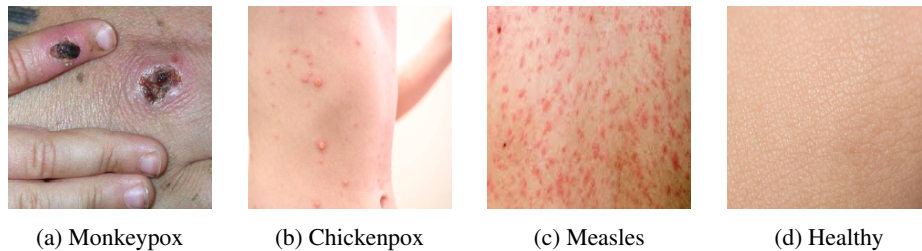


Fig. 4: Samples from the MSID [14] dataset. (a) Monkeypox: firm pustules with umbilication and surrounding erythema. (b) Chickenpox: fragile vesicles at different stages. (c) Measles: diffuse erythematous maculopapular rash. (d) Healthy: skin without visible lesions or inflammation.

Although MSID was later expanded to over 8,600 samples through aggressive augmentation, our experiments rely solely on the original, unaugmented images. The dataset features images from various anatomical regions and lighting conditions, adding to its robustness and clinical realism. MSID is positioned as an intermediate-complexity

dataset for 4-way classification, bridging the binary structure of MSLD v1.0 and the more complex MSLD v2.0.

Dataset Limitations: The datasets suffer from inherent class imbalance and limited coverage of skin tone diversity, both of which constrain model performance on underrepresented categories. In particular, MSLD v1.0 and MSID contain only a small number of samples for certain diseases, while MSLD v2.0, despite being larger, still exhibits uneven distribution across conditions. Furthermore, as all datasets are primarily sourced from publicly available web repositories, they lack racial and geographic diversity. These limitations not only reduce the reliability of accuracy estimates for minority classes but also raise concerns about the robustness and fairness of model generalization to real-world clinical populations.

2.2 Preprocessing

To ensure architectural compatibility and maintain experimental consistency, all input images were resized to 128×128 for consistent feature extraction. No additional preprocessing or data augmentation techniques were applied. This deliberate choice was made to isolate the true representation capability of each CNN backbone, without confounding the results with synthetic variability introduced through augmentation. By maintaining the original (resized-only) image content, we ensure a fair and controlled comparison of feature extraction quality across models. Each resized image was directly passed through the corresponding backbone network to extract deep feature embeddings, which were subsequently used as input to the downstream few-shot classifier.

2.3 Feature Extraction via CNN Backbones

Our pipeline begins by extracting feature embeddings from input images using one of six widely adopted CNN backbones: VGG16, InceptionV3, ResNet50, DenseNet121, MobileNetV2_100, and EfficientNet B1. Each model is initialized with ImageNet pre-trained weights and kept entirely frozen during inference to ensure a fair and unbiased comparison across architectures. Feature maps are taken from the final convolutional layer of each network, producing a tensor of shape (B, C, H', W') for a batch of B images. We then apply a `SelectAdaptivePool2d` operation, which compresses each spatial feature map to shape (B, C) as shown in Equation 1 and passed directly to the `SimpleShot` classifier.

Let $\mathbf{F} \in \mathbb{R}^{B \times C \times H' \times W'}$ be the feature maps obtained from the last convolutional layer of a CNN. The adaptive pooling operation \mathcal{P} reduces spatial dimensions such that:

$$\mathcal{P}(\mathbf{F}) = \frac{1}{H'W'} \sum_{i=1}^{H'} \sum_{j=1}^{W'} \mathbf{F}_{::,i,j} \in \mathbb{R}^{B \times C \times 1 \times 1} \quad (1)$$

This pooled tensor is then reshaped to $\mathbb{R}^{B \times C}$ to obtain a (B, C) feature matrix before being passed to the `SimpleShot` classifier.

This process ensured that all embeddings, regardless of backbone architecture, had consistent structure and were spatially invariant, allowing a fair comparison of their representational power for few-shot classification.

2.4 Few-shot Classification via SimpleShot

For all classification tasks, we employed SimpleShot [52], a non-parametric and inductive few-shot learning algorithm that requires no meta-training. SimpleShot operates by computing class prototypes from the support set and classifying query samples via nearest-centroid matching in a normalized embedding space. Its simplicity, efficiency, and strong baseline performance make it an ideal choice for evaluating the representational power of CNN-based feature extractors without introducing algorithm-specific learning biases. Furthermore, follow-up studies have shown that SimpleShot is the best-performing non-parametric and inductive FSL method in challenging cross-domain few-shot settings [44], often outperforming more complex meta-learning approaches while maintaining minimal computational overhead. This makes it particularly well-suited as a standardized backbone evaluation tool in our low-data clinical scenario.

Each experiment follows an N -way M -shot protocol, where $N \in \{2, 4, 6\}$ varies by dataset and $M \in \{1, 5, 10\}$ defines the number of support examples per class. For each classification episode, a support set is randomly sampled with M labeled examples per class, while a fixed query set of 50 images is used for evaluation. Every configuration is repeated over 100 randomly sampled episodes, and mean accuracy with 95% confidence intervals is reported to ensure statistical robustness.

Let $\mathbf{z}_i \in \mathbb{R}^C$ denote the embedding of a support sample and let \mathcal{S}_c be the set of support embeddings for class c . The prototype for class c is computed as the mean of its support embeddings:

$$\mathbf{p}_c = \frac{1}{|\mathcal{S}_c|} \sum_{\mathbf{z}_i \in \mathcal{S}_c} \mathbf{z}_i, \quad (2)$$

where $\mathbf{p}_c \in \mathbb{R}^C$ is the class prototype. During inference, query samples are classified to the nearest prototype we get from Equation 2 in the normalized embedding space. This formulation ensures consistent evaluation across varying task complexities and support sizes, enabling systematic assessment of feature extractor generalizability under different levels of class granularity and data scarcity.

2.5 Evaluation Metrics

Model performance was evaluated using the mean classification accuracy across 100 independently sampled few-shot classification tasks for each configuration. All experiments were conducted using Google Colab on a single NVIDIA T4 GPU. To quantify the statistical reliability of each result, we computed 95% confidence intervals using the `mean_confidence_interval` function, which estimates the interval based on the Student’s t-distribution. Formally, each result is reported as $\mu \pm t_{n-1} \cdot \frac{\sigma}{\sqrt{n}}$; where μ is the sample mean accuracy, σ is the sample standard deviation, $n = 100$ is the number of episodes, and t_{n-1} is the critical value of the t-distribution with $n - 1$ degrees of freedom at 95% confidence. The reporting format captures both central tendency and variability across episodes, enabling robust comparisons across backbones, datasets, and shot configurations.

3 Results and Discussion

This section presents our experimental results and insights, where we begin by benchmarking multiple CNN backbones across datasets of increasing complexity. Next, we quantify the impact of increasing support set size (N -shot) on classification accuracy. Furthermore, we analyze the class-wise performance using the best-performing model and provide a thorough analysis of cross-dataset generalization.

3.1 Backbone Comparison Across Datasets

Table 1 reports the average classification accuracy (with 95% confidence intervals) for six CNN models across three datasets under 1-shot, 5-shot, and 10-shot conditions.

Table 1: Performance analysis of proposed pipeline with different CNN feature extractors across different datasets.

Backbone	6-way (MSLD v2.0)			4-way (MSID)			2-way (MSLD v1.0)		
	10-shot	5-shot	1-shot	10-shot	5-shot	1-shot	10-shot	5-shot	1-shot
MobileNet v2_100	0.624 ± 0.006	0.539 ± 0.007	0.351 ± 0.010	0.696 ± 0.008	0.609 ± 0.011	0.443 ± 0.015	0.674 ± 0.010	0.642 ± 0.013	0.548 ± 0.017
VGG16	0.566 ± 0.006	0.516 ± 0.008	0.358 ± 0.011	0.641 ± 0.008	0.579 ± 0.010	0.440 ± 0.014	0.710 ± 0.011	0.676 ± 0.011	0.599 ± 0.018
EfficientNet_B1	0.537 ± 0.007	0.459 ± 0.008	0.296 ± 0.009	0.632 ± 0.008	0.553 ± 0.009	0.411 ± 0.014	0.644 ± 0.009	0.618 ± 0.012	0.567 ± 0.017
DenseNet121	0.523 ± 0.006	0.450 ± 0.009	0.305 ± 0.009	0.606 ± 0.009	0.523 ± 0.010	0.389 ± 0.014	0.634 ± 0.012	0.604 ± 0.014	0.531 ± 0.015
ResNet50	0.498 ± 0.007	0.431 ± 0.010	0.288 ± 0.010	0.548 ± 0.009	0.475 ± 0.010	0.359 ± 0.012	0.643 ± 0.011	0.598 ± 0.013	0.533 ± 0.015
InceptionV3	0.336 ± 0.006	0.288 ± 0.007	0.213 ± 0.007	0.397 ± 0.008	0.344 ± 0.007	0.282 ± 0.007	0.578 ± 0.010	0.556 ± 0.011	0.496 ± 0.011

Across nearly all experimental configurations, MobileNetV2_100 consistently outperforms other CNN backbones, underscoring its strong generalization capability and making it particularly well-suited for low-data regimes common in few-shot learning scenarios. We observe a clear positive correlation between the number of support examples and classification accuracy, reaffirming that increasing the number of labeled instances enhances the model’s ability to learn discriminative features. However, task complexity plays a significant role in performance degradation as the classification challenge shifts from 2-way to 6-way settings, accuracy drops considerably, likely due to increased inter-class visual similarity and ambiguity. Interestingly, larger or deeper models such as InceptionV3 and VGG16 do not necessarily yield superior results, often underperforming compared to more compact architectures. This suggests that lightweight models with effective inductive biases may be more advantageous than computationally heavier counterparts in the context of few-shot learning.

To substantiate these findings, we also report inference time, parameter count, and floating point operations (FLOPs) for each backbone in Table 2. MobileNetV2_100

Table 2: Efficiency metrics of different backbone models evaluated on a single NVIDIA T4 GPU. Parameters are in millions (M), FLOPs in millions (M), and inference time per image in milliseconds (ms/img).

Backbone	Parameters (M)	FLOPs (M)	Inference Time (ms/img)
MobileNetV2_100	1.81	186.42	2.84
VGG16	14.71	10,060	7.66
EfficientNet_B1	6.10	365.04	15.32
DenseNet121	6.95	1,872.64	19.33
ResNet50	23.51	2,700	7.38
InceptionV3	21.79	1,468.72	15.44

achieves the lowest latency and computational cost while maintaining superior accuracy, reinforcing its suitability for deployment in resource-constrained environments.

3.2 Impact of N-Shot Scaling

To further investigate the influence of support set size, we conducted a 6-way classification experiment using MobileNetV2_100. Figure 5 illustrates the accuracy trend as N increases from 1 to 10. We observe a significant performance gain between 1-shot and 5-shot settings, with a more gradual improvement from 5 to 10 shots. These results are consistent with existing FSL literature, wherein larger support sets facilitate more robust decision boundaries by reducing intra-class variance.

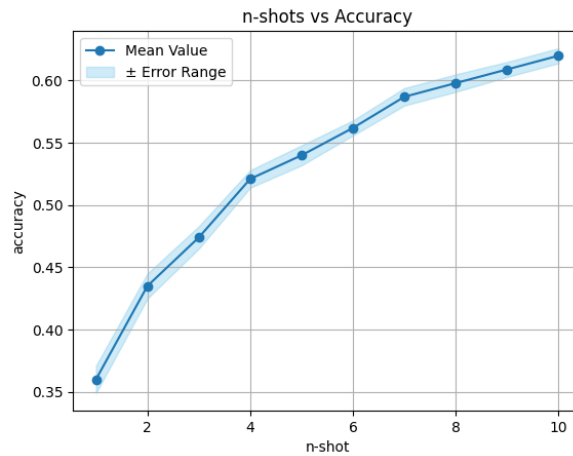


Fig. 5: Accuracy improvement with increasing support size on the 6-way classification task (Error bars represent 95% confidence intervals).

3.3 Per-Class Classification Performance

We assessed class-wise accuracy using `MobileNetV2_100` under 2-way, 4-way, and 6-way settings (Figure 6). While other classes consistently achieve high accuracy, Monkeypox performance drops notably in the 6-way task. To investigate this decline, we analyzed the confusion matrix (Figure 7), which reveals substantial misclassifications between Monkeypox, Chickenpox, Cowpox, and HFMD. This pattern reflects the strong visual overlap among these conditions, where lesions share similar morphology and distribution. These findings highlight the inherent difficulty of distinguishing visually related diseases in low-data diagnostic settings.

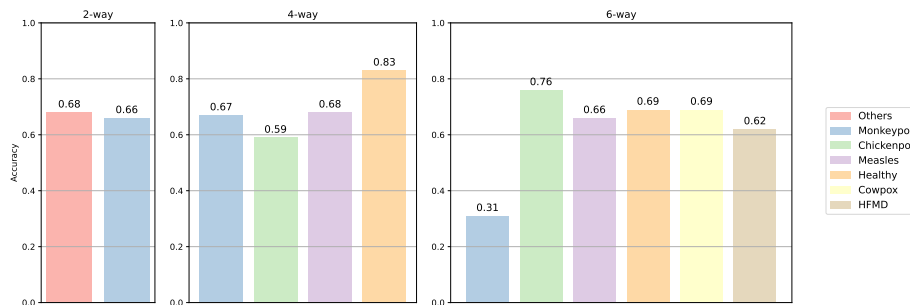


Fig. 6: Class-wise accuracy using the `MobileNetV2_100` backbone across 2-way, 4-way, and 6-way tasks. Accuracy for Monkeypox decreases as the number of classes increases, indicating greater inter-class confusion in more complex settings.

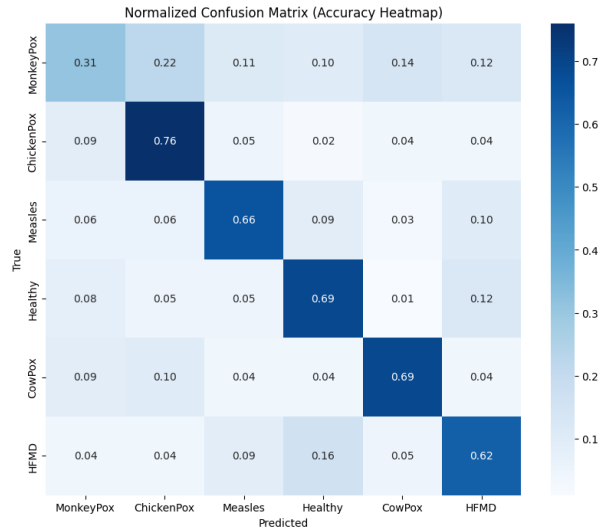


Fig. 7: Confusion matrix on the 6-way MSLD v2.0 task (10-shot). Misclassifications are concentrated among visually similar diseases, highlighting inter-class confusion.

3.4 Cross-Dataset Generalization

We conducted cross-dataset experiments between MSLD v2.0 and MSID to evaluate robustness under domain shift, where prototypes were constructed using one dataset (support set) and classification was performed on the other (query set). Results are summarized in Table 3.

While using the full 6-class MSLD v2.0 support set to classify MSID queries, accuracy dropped sharply to around 44%, compared to in-domain results above 60%, highlighting the severity of domain shift. Restricting evaluation to the four overlapping classes yielded much more stable results, with performance converging near 57%–58% regardless of which dataset provided the support set. In the binary Mpox-vs-Others setting, cross-dataset transfer was more reliable, reaching about 63%–68% accuracy depending on the direction. These findings show that while cross-dataset generalization is feasible, domain differences substantially affect multi-class performance. The results further suggest that simpler binary diagnostic setups are more robust, while higher-way classification remains vulnerable to inter-dataset discrepancies.

Table 3: Cross-dataset few-shot classification accuracy (mean \pm 95% CI). Support and query sets are drawn from different datasets to assess generalization.

Experiment Type	Support Set	Query Set	Accuracy
In-domain (baseline)	MSLD v2.0 (6-way)	MSLD v2.0 (6-way)	0.624 \pm 0.006
	MSID (4-way)	MSID (4-way)	0.696 \pm 0.008
Cross-dataset (mismatch)	MSLD v2.0 (6-way)	MSID (4-way)	0.444 \pm 0.009
Cross-dataset (4-class overlap)	MSLD v2.0 (4-way)	MSID (4-way)	0.570 \pm 0.009
	MSID (4-way)	MSLD v2.0 (4-way)	0.578 \pm 0.011
Cross-dataset (binary Mpox vs Others)	MSLD v2.0 (2-way)	MSID (2-way)	0.679 \pm 0.016
	MSID (2-way)	MSLD v2.0 (2-way)	0.631 \pm 0.010

4 Conclusion

We evaluate six CNN backbones for few-shot classification of Monkeypox and pox-like skin diseases. Across three datasets and multiple task complexities, `MobileNetV2_100` achieves the best balance of accuracy and efficiency. Performance improves substantially from 1-shot to 5-shot settings, with limited gains beyond that. Per-class analysis shows persistent confusion among visually similar diseases, highlighting the importance of backbone selection. Cross-dataset experiments indicate that binary Mpox-vs-Others transfer remains relatively stable (63–68%), whereas multi-class generalization declines under domain shift, underscoring the need for domain-adaptive strategies. These results demonstrate the practical value of lightweight CNNs with inductive few-shot methods, and future work may explore self-supervised pretraining and domain adaptation to enhance robustness across clinical datasets.

References

1. Abrar, A., Tabassum, F., Ahmed, S.: Performance evaluation of large language models in bangla consumer health query summarization. In: 2024 27th International Conference on Computer and Information Technology (ICCIT). pp. 2748–2753 (2024) [2](#)
2. Ahamed, M., Kabir, R.B., Dipto, T.T., Al Mushabbir, M., Ahmed, S., Kabir, M.H.: Performance analysis of few-shot learning approaches for bangla handwritten character and digit recognition. In: 2024 6th International Conference on Sustainable Technologies for Industry 5.0 (STI). pp. 1–6 (2024) [2](#)
3. Ahmed, S., Hasan, M.B., Ahmed, T., Kabir, M.H.: DExNet: Combining observations of domain adapted critics for leaf disease classification with limited data (2025) [2](#)
4. Ahmed, S., Hasan, M.B., Ahmed, T., Sony, M.R.K., Kabir, M.H.: Less is more: Lighter and faster deep neural architecture for tomato leaf disease classification. *IEEE Access* **10**, 68868–68884 (2022) [2](#)
5. Ahmed, T., Hasan, M.B., Ahmed, S., Kabir, M.H.: ExE-Net: Explainable ensemble network for potato leaf disease classification. In: 2024 IEEE Canadian Conference on Electrical and Computer Engineering (CCECE). pp. 335–339 (2024) [2](#)
6. Ahmed, T., Ivan, S., Munir, A., Ahmed, S.: Decoding depression: Analyzing social network insights for depression severity assessment with transformers and explainable ai. *Natural Language Processing Journal* **7**, 100079 (2024) [2](#)
7. Ahmed, T., Munir, A., Ahmed, S., Hasan, M.B., Reza, M.T., Kabir, M.H.: Structure-enhanced translation from pet to ct modality with paired gans. In: Proceedings of the 2023 6th International Conference on Machine Vision and Applications. p. 142–146. ICMVA '23, Association for Computing Machinery, New York, NY, USA (2023) [2](#)
8. Al-Musa, A., Chou, J., LaBere, B.: The resurgence of a neglected orthopoxvirus: Immunologic and clinical aspects of monkeypox virus infections over the past six decades. *Clinical Immunology (Orlando, Fla.)* **243**, 109108–109108 (2022) [2](#)
9. Ali, S.N., Ahmed, M.T., Jahan, T., Paul, J., Sani, S.M.S., Noor, N., Asma, A.N., Hasan, T.: A web-based mpox skin lesion detection system using state-of-the-art deep learning models considering racial diversity (2023) [2](#), [3](#), [4](#), [5](#), [6](#)
10. Ali, S.N., Ahmed, M.T., Paul, J., Jahan, T., Sani, S.M.S., Noor, N., Hasan, T.: Monkeypox skin lesion detection using deep learning models: A feasibility study (2022) [2](#), [3](#), [4](#), [5](#)
11. Arif, N.H., Rabby, S., Papon, M.H.H., Ahmed, S.: Preemptive hallucination reduction: An input-level approach for multimodal language model (2025) [2](#)
12. Ashikur Rahman, A.B.M., Hasan, M.B., Ahmed, S., Ahmed, T., Ashmafee, M.H., Kabir, M.R., Kabir, M.H.: Two decades of bengali handwritten digit recognition: A survey. *IEEE Access* **10**, 92597–92632 (2022) [2](#)
13. Aziz, S., Arif, N.H., Ahabab, S., Ahmed, S., Ahmed, T., Kabir, M.H.: Improved speech emotion recognition in bengali language using deep learning. In: 2023 26th International Conference on Computer and Information Technology (ICCIT). pp. 1–6 (2023) [2](#)
14. Bala, D., Hossain, M.S., Hossain, M.A., Abdullah, M.I., Rahman, M.M., Manavalan, B., Gu, N., Islam, M.S., Huang, Z.: Monkeynet: A robust deep convolutional neural network for monkeypox disease detection and classification. *Neural Networks* **161** (2023) [2](#), [3](#), [4](#), [5](#), [6](#)
15. Cai, A., Hu, W., Zheng, J.: Few-shot learning for medical image classification. In: Farkaš, I., Masulli, P., Wermter, S. (eds.) *Artificial Neural Networks and Machine Learning – ICANN 2020*. pp. 441–452. Springer International Publishing, Cham (2020) [2](#)
16. Cassidy, B., Kendrick, C., Brodzicki, A., Jaworek-Korjakowska, J., Yap, M.H.: Analysis of the isic image datasets: Usage, benchmarks and recommendations. *Medical image analysis* **75**, 102305 (2021) [2](#)

17. Chen, B., Han, Y., Yan, L.: A few-shot learning approach for monkeypox recognition from a cross-domain perspective. *Journal of biomedical informatics* p. 104449 (2023) [3](#)
18. Dai, Z., Yi, J., Yan, L., Xu, Q., Hu, L., Zhang, Q., Li, J., Wang, G.: Pfemed: Few-shot medical image classification using prior guided feature enhancement. *Pattern Recognition* (2023) [2](#)
19. Deng, J., Liu, J., Kong, C., Zang, B., Hu, Y., Zou, M.: Using novel deep learning models for rapid and efficient assistance in monkeypox screening from skin images. *Frontiers in Medicine* **11** (2024) [2](#)
20. Fuad, T.R., Ahmed, S., Ivan, S.: Aqua20: A benchmark dataset for underwater species classification under challenging conditions (2025) [2](#)
21. Haque, M.E., Ahmed, M.R., Nila, R., Islam, S.: Classification of human monkeypox disease using deep learning models and attention mechanisms. *ArXiv* **abs/2211.15459** (2022) [2](#)
22. Hasan, M.B., Ahmed, T., Ahmed, S., Kabir, M.H.: Gaitcgn++: Improving gcn-based gait recognition with part-wise attention and dropgraph. *Journal of King Saud University - Computer and Information Sciences* **35**(7), 101641 (2023) [2](#)
23. He, K., Zhang, X., Ren, S., Sun, J.: Deep residual learning for image recognition (2015) [3](#)
24. Huang, G., Liu, Z., van der Maaten, L., Weinberger, K.Q.: Densely connected convolutional networks (2018) [3](#)
25. Islam, A., G., M., El, E.S.M., Moustafa, H.E.D.: Medical image classification for monkeypox case using deep learning algorithms: A survey. *Journal of Artificial Intelligence and Metaheuristics* (2023) [2](#)
26. Ivan, S., Ahmed, T., Ahmed, S., Kabir, M.H.: A vision-language multimodal framework for detecting hate speech in memes. In: 2024 IEEE Canadian Conference on Electrical and Computer Engineering (CCECE). pp. 464–468 (2024) [2](#)
27. Jiang, H., Gao, M., Li, H., Jin, R., Miao, H., Liu, J.: Multi-learner based deep meta-learning for few-shot medical image classification. *IEEE Journal of Biomedical and Health Informatics* **27**, 17–28 (2022) [2](#)
28. Khan, A.M., Ashrafee, A., Khan, F.S., Hasan, M.B., Kabir, M.H.: Attresdu-net: Medical image segmentation using attention-based residual double u-net. In: 2023 International Joint Conference on Neural Networks (IJCNN). pp. 1–8 (2023) [2](#)
29. Khan, A.M., Ashrafee, A., Sayera, R., Ivan, S., Ahmed, S.: Rethinking cooking state recognition with vision transformers. In: 25th International Conference on Computer and Information Technology (ICCIT). pp. 170–175 (2022) [2](#)
30. Khan, A., Kamal, F., Chowdhury, M.A., Ahmed, T., Laskar, M.T.R., Ahmed, S.: BanglaCHQ-summ: An abstractive summarization dataset for medical queries in Bangla conversational speech. In: Proceedings of the First Workshop on Bangla Language Processing (BLP-2023). pp. 85–93. Association for Computational Linguistics, Singapore (Dec 2023) [2](#)
31. Khan, A., Kamal, F., Nower, N., Ahmed, T., Ahmed, S., Chowdhury, T.: NERvous about my health: Constructing a Bengali medical named entity recognition dataset. In: Findings of the Association for Computational Linguistics: EMNLP 2023. pp. 5768–5774. Association for Computational Linguistics, Singapore (Dec 2023) [2](#)
32. Kottath, A.V., P, R.: Poxltnet50: Deep learning-based approach for accurate image detection of monkeypox disease. *Journal of Innovative Image Processing* (2025) [2](#)
33. Kundu, D., Rahman, M.M., Rahman, A., Das, D., Siddiqi, U.R., Alam, M.G.R., Dey, S.K., Muhammad, G., Ali, Z.: Federated deep learning for monkeypox disease detection on gan-augmented dataset. *IEEE Access* **12**, 32819–32829 (2024) [2](#)
34. Liu, B., Yu, X., Yu, A., Zhang, P., Wan, G., Wang, R.: Deep few-shot learning for hyperspectral image classification. *IEEE Transactions on Geoscience and Remote Sensing* **57**, 2290–2304 (2019) [2](#)
35. Mahbub, R., Khan, I., Anuva, S., Shahriar, M.S., Laskar, M.T.R., Ahmed, S.: Unveiling the essence of poetry: Introducing a comprehensive dataset and benchmark for poem sum-

- marization. In: Proceedings of the Conference on Empirical Methods in Natural Language Processing, pp. 14878–14886. Association for Computational Linguistics (2023) [2](#)
36. McCollum, A., Shelus, V.S., Hill, A., Traore, T., Onoja, B., Nakazawa, Y., Doty, J.B., Yinka-Ogunleye, A., Petersen, B., Hutson, C., Lewis, R.F.: Epidemiology of human mpox — worldwide, 2018–2021. *Morbidity and Mortality Weekly Report* **72**, 68–72 (2023) [2](#)
 37. Mitjà, O., Ogoina, D., Titanji, B.K., Galván, C., Muyembe, J.J., Marks, M., Orkin, C.: Monkeypox. *Lancet (London, England)* **401**, 60–74 (2022) [1](#)
 38. Nisar, H., Saleem, O., Sapna, F., Sham, S., Perakash, R.S., Kiran, N., Anjali, F., Mehreen, A., Ram, B.: A narrative review on the monkeypox virus: An ongoing global outbreak hitting the non-endemic countries. *Cureus* **15** (2023) [2](#)
 39. Ouyang, C., Biffi, C., Chen, C., Kart, T., Qiu, H., Rueckert, D.: Self-supervised learning for few-shot medical image segmentation. *IEEE Transactions on Medical Imaging* **41** (2022) [2](#)
 40. Parums, D.: Editorial: Current status of non-endemic global infections with the monkeypox virus. *Medical Science Monitor : International Medical Journal of Experimental and Clinical Research* **28**, e938203–1 – e938203–3 (2022) [2](#)
 41. Quarleri, J., Delpino, M., Galvan, V.: Monkeypox: considerations for the understanding and containment of the current outbreak in non-endemic countries. *GeroScience* **44** (2022) [2](#)
 42. Raiyan, S.R., Amio, Z.Z., Ahmed, S.: HaSPeR: An image repository for hand shadow puppet recognition. In: ICCV 2025 Workshop on Cultural Continuity of Artists (2025) [2](#)
 43. Sandler, M., Howard, A., Zhu, M., Zhmoginov, A., Chen, L.C.: Mobilenetv2: Inverted residuals and linear bottlenecks (2019) [3](#)
 44. Sekhar, A., Bhattacharya, A., Goyal, V., Goel, V., Bhangale, A., Gupta, R.K., Sethi, A.: Cross-domain evaluation of few-shot classification models: Natural images vs. histopathological images (2024) [8](#)
 45. Shafaati, M., Zandi, M.: State-of-the-art on monkeypox virus: an emerging zoonotic disease. *Infection* **50**, 1425–1430 (2022) [2](#)
 46. Simonyan, K., Zisserman, A.: Very deep convolutional networks for large-scale image recognition (2015) [3](#)
 47. Singh, R., Bharti, V., Purohit, V., Kumar, A., Singh, A.K., Singh, S.K.: Metamed: Few-shot medical image classification using gradient-based meta-learning. *Pattern Recognition* **120**, 108111 (2021) [2](#)
 48. Szegedy, C., Vanhoucke, V., Ioffe, S., Shlens, J., Wojna, Z.: Rethinking the inception architecture for computer vision (2015) [3](#)
 49. Tabassum, F., Islam, S., Rizwan, S., Sobhan, M., Ahmed, T., Ahmed, S., Chowdhury, T.M.: Precision cancer classification and biomarker identification from mrna gene expression via dimensionality reduction and explainable ai (2024) [2](#)
 50. Tan, M., Le, Q.V.: Efficientnet: Rethinking model scaling for convolutional neural networks (2020) [3](#)
 51. Wang, T.Y., Song, Y., Cai, P., Sahoo, J.P., Mondal, S.: A comprehensive survey of few-shot learning: Evolution, applications, challenges, and opportunities. *ACM Computing Surveys* **55**, 1–40 (2022) [2](#)
 52. Wang, Y., Chao, W.L., Weinberger, K.Q., van der Maaten, L.: Simpleshot: Revisiting nearest-neighbor classification for few-shot learning. *arXiv:1911.04623* (2019) [3](#), [4](#), [8](#)
 53. Wang, Y., Yao, Q.: Few-shot learning: A survey. *ArXiv* **abs/1904.05046** (2019) [2](#)
 54. Yasmeen, A., Rahman, F.I., Ahmed, S., Kabir, M.H.: Csvc-net: Code-switched voice command classification using deep cnn- lstm network. In: 2021 Joint 10th International Conference on Informatics, Electronics & Vision (ICIEV) and 2021 5th International Conference on Imaging, Vision & Pattern Recognition (icIVPR). pp. 1–8 (2021) [2](#)
 55. Zhang, B., Gao, B., Liang, S., Li, X., Wang, H.: A classification algorithm based on improved meta learning and transfer learning for few-shot medical images. *IET Image Process.* **17**, 3589–3598 (2023) [2](#)